ARTICLE
Journal of Cellular Biochemistry 106:127–138 (2009)

Journal of Cellular Biochemistry

Matrix Vesicles Originate From Apical Membrane Microvilli of Mineralizing Osteoblast-Like Saos-2 Cells

Cyril Thouverey,[1,2,3,4,5,6] Agnieszka Strzelecka-Kiliszek,[1] Marcin Balcerzak,[1] René Buchet,[2,3,4,5,6] and Slawomir Pikula[1*]

[1]*Department of Biochemistry, Nencki Institute of Experimental Biology, Polish Academy of Sciences, PL-02093 Warsaw, Poland*

[2]*Université de Lyon, Villeurbanne F-69622, France*

[3]*Université Lyon 1, Villeurbanne F-69622, France*

[4]*INSA de Lyon, Villeurbanne F-69621, France*

[5]*CPE Lyon, Villeurbanne F-69616, France*

[6]*ICBMS CNRS UMR 5246, Villeurbanne F-69622, France*

ABSTRACT

In bone, mineralization is tightly regulated by osteoblasts and hypertrophic chondrocytes which release matrix vesicles (MVs) and control extracellular ionic conditions and matrix composition. MVs are the initial sites of hydroxyapatite (HA) mineral formation. Despite growing knowledge about their morphology and function, their biogenesis is not well understood. The purpose of this work was to determine the source of MVs in osteoblast lineage, Saos-2 cells, and to check whether MVs originated from microvilli. Microvilli were isolated from the apical plasma membrane of Saos-2 cells. Their morphology, structure, and function were compared with those of MVs. The role of actin network in MV release was investigated by using microfilament perturbing drugs. When examined by electron microscopy MVs and microvillar vesicles were found to exhibit similar morphology with trilaminar membranes and diameters in the same range. Both types of vesicles were able to induce HA formation. Their electrophoretic profiles displayed analogous enrichment in alkaline phosphatase, Na^+/K^+ ATPase, and annexins A2 and A6. MVs and microvillar vesicles exhibited almost the same lipid composition with a higher content of cholesterol, sphingomyelin, and phosphatidylserine as compared to plasma membrane. Finally, cytochalasin D, which inhibits actin polymerization, was found to stimulate release of MVs. Our findings were consistent with the hypothesis that MVs originated from cell microvilli and that actin filament disassembly was involved in their biogenesis. J. Cell. Biochem. 106: 127–138, 2009.

KEY WORDS: MATRIX VESICLES; ORIGIN; Saos-2 CELLS; MINERALIZATION

Bone is a complex, dynamic, highly specialized form of connective tissue that together with cartilage makes up the skeleton. Bone matrix is composed of an organic phase, containing mostly type-I collagen, providing tensile strength, and of an inorganic phase, hydroxyapatite (HA), which gives it mechanical resistance [Buckwalter and Cooper, 1987]. Osteoclasts, osteoblasts, and osteocytes are the three major cell types present in bone. Plasticity of the skeleton and its ability to adapt relies on continuous modeling and remodeling that require osteoclastic resorption of bone matrix and deposition of a newly mineralized matrix by

Abbreviations used: AA, ascorbic acid; AnxA6, annexin A6; AR-S, Alizarin Red-S; β-GP, β-glycerophosphate; CCD, cytochalasin D; CHOL, cholesterol; DAGs, diacylglycerols; FACS, fluorescence activated cell sorter; FBS, fetal bovine serum; FFAs, free fatty acids; FITC, fluorescein isothiocyanate; HA, hydroxyapatite; HBSS, Hank's balanced salt solution; MAGs, monoacylglycerols; MVs, matrix vesicles; PA, phosphatidic acid; PAGE, polyacrylamide gel electrophoresis; PBS, phosphate-buffered saline; PC, phosphatidylcholine; PE, phosphatidylethanolamine; PHL, phalloidin, PI, phosphatidylinositol; P_i, inorganic phosphate, PP_i, inorganic pyrophosphate; PS, phosphatidylserine; SDS, sodium dodecyl sulfate; SM, sphingomyelin; TAGs, triacylglycerols; TNAP, tissue non-specific alkaline phosphatase; TBS, Tris-buffered saline; TRITC, tetramethylrhodamine isothiocyanate.

Grant sponsor: Polish Ministry of Science and Higher Education; Grant number: N301 025 32/1120; Grant sponsor: Polonium; Grant number: 05819NF; Grant sponsor: CNRS (France); Grant sponsor: The Rhône-Alpes region (France).

*Correspondence to: Professor Slawomir Pikula, Department of Biochemistry, Nencki Institute of Experimental Biology, Polish Academy of Sciences, 3 Pasteur Street, 02-093 Warsaw, Poland. E-mail: s.pikula@nencki.gov.pl

Received 7 April 2008; Accepted 8 October 2008 • DOI 10.1002/jcb.21992 • 2008 Wiley-Liss, Inc.

Published online 13 November 2008 in Wiley InterScience (www.interscience.wiley.com).

osteoblasts [Marks and Popoff, 1988]. Osteocytes maintain the osseous matrix, participate in extracellular exchanges and are involved in the mechanotransduction [Marks and Popoff, 1988]. Bone mineralization occurs during the formation, development, remodeling, and repair of the osseous tissue [Thouverey et al., 2007; Van de Lest and Vaandrager, 2007]. Thus, osseous mineralization is initiated by two types of cells: hypertrophic chondrocytes during endochondral ossification and osteoblasts during intramembranous and haversian ossification. The regulation of physiological mineralization is mediated at cellular and tissue levels, and requires coordination between stimulatory and inhibitory factors [Van de Lest and Vaandrager, 2007]. Osteoblasts are fusiform, cuboidal, polyhedral, or spherical cells located at the surface of a forming bone. These cells are polarized with the basolateral plasma membrane facing the bone marrow and the apical plasma membrane facing the forming bone [Ilvesaro et al., 1999]. Osteoblasts, such as odontoblasts and hypertrophic chondrocytes, participate in the synthesis of extracellular matrix proteins and in matrix mineralization by releasing matrix vesicles (MVs) [Anderson, 1969, 1995, 2003; Balcerzak et al., 2003]. Calcifying cells were shown to accumulate inorganic phosphate (P_i) in their cytoplasm [Wuthier et al., 1977] as well as high levels of Ca^{2+} ions in their mitochondria [Brighton and Hunt, 1976] prior to mineralization. Mitochondrial Ca^{2+} ions are released and, in combination with high levels of P_i, form amorphous calcium phosphate at sites of MV formation [Wu et al., 1995]. Extracellular MVs promote HA formation from these immature minerals in their lumen [Wuthier, 1975a]. Then, MV phospholipases [Wu et al., 2002; Balcerzak et al., 2007] together with the HA crystals contribute to the breakdown of the MV membrane leading to the release of the MV content into the extracellular matrix where mineralization is propagated [Anderson, 1995]. Despite growing knowledge about the structure and functions of MVs, little is known about the mechanism of their biogenesis, especially from osteoblasts. It has been demonstrated that MVs originate from the plasma membrane of hypertrophic chondrocytes [Rabinovitch and Anderson, 1976; Wuthier et al., 1977]. Four hypotheses have been proposed concerning the mechanisms of MV formation [Rabinovitch and Anderson, 1976]. As areas of mineralization coincide with chondrocyte apoptosis in growth plate cartilages, it was suggested that MVs arise as a result of the rearrangement of the apoptotic cell membrane [Kardos and Hubbard, 1982]. This was not confirmed by Kirsch et al. [2003] who showed that MVs and the apoptotic bodies are structurally and functionally different. However, it should be noted that MV formation and apoptosis probably occur concomitantly during the cell differentiation process. Indeed, only mature (but not immature) osteoblasts mineralize their matrix, while only terminally differentiated growth plate chondrocytes release MVs [Kirsch, 2007]. Electron microscopy observations indicated that MVs could be formed by extrusion of preformed cytoplasmic structures into the extracellular matrix [Akisaka and Shigenaga, 1983; Akisaka et al., 1988]. Rabinovitch and Anderson [1976], although identifying other possible mechanisms for MV biogenesis, favored, above all, the budding of MVs from cellular processes. Then, the last hypothesis was confirmed by freeze-fracture electron microscopy [Borg et al., 1978, 1981; Cecil and Anderson, 1978] showing that the topology of MVs is not changed from that of the parent cell (i.e., there is no inside-out inversion of the membrane). Anderson and Reynolds [1973] were the first to suggest that MVs arise by polarized apical budding from mineralization-competent cells. Later, Cecil and Anderson [1978] demonstrated that MVs appear to bud from the tips of plasma membrane processes of hypertrophic chondrocytes. Furthermore, MVs may arise from the membrane adjacent to the newly formed extracellular matrix [Morris et al., 1992]. Cell surface microvilli of hypertrophic chondrocytes were found to be the precursors of MVs and the actin network appeared to be essential for their formation [Hale et al., 1983; Hale and Wuthier, 1987].

The aim of this work was to check whether MVs originate from microvilli of the osteoblast lineage, as in the case of hypertrophic chondrocytes. Several models of organ (embryonic bone) or cell (chondrocytes) cultures have been used to study mineralization and MV biogenesis [Anderson and Reynolds, 1973; Golub et al., 1983; Anderson et al., 1990; Garimella et al., 2004]. Human osteosarcoma Saos-2 cells undergo the entire osteoblastic differentiation program from proliferation to mineralization [Hausser and Brenner, 2004], produce a collagenous extracellular matrix [McQuillan et al., 1995] and spontaneously release mineralization-competent MVs [Fedde, 1992]. Therefore, we selected Saos-2 cell cultures as a convenient model of osteoblastic mineralization to analyze the mechanisms involved in the release of MVs into the extracellular matrix. To this end, microvilli from apical Saos-2 cell plasma membrane were purified. Their protein and lipid compositions as well as their ability to mineralize were compared with those of MVs. The role of actin network in MV formation was investigated by using two drugs which affect microfilament polymerization and depolymerization [Hale and Wuthier, 1987]. Our findings confirmed that mineralizing osteoblast-like Saos-2 cells are polarized and that microvilli from the apical plasma membrane are sites of origin of MVs. Moreover, the actin network depolymerization was found to enhance MV release from Saos-2 cells.

MATERIALS AND METHODS

CELL CULTURE AND STIMULATION FOR MINERALIZATION

Human osteosarcoma Saos-2 cells (ATCC HTB-85) were cultured in McCoy's 5A (ATCC) supplemented with 100 U/ml penicillin, 100 μg/ml streptomycin (both from Sigma), and 15% fetal bovine serum (FBS, v/v; Gibco). The mineralization was induced by culturing the confluent cells (7 days to reach confluence) in growth medium supplemented with 50 μg/ml ascorbic acid (AA; Sigma) and 7.5 mM β-glycerophosphate (β-GP; Sigma) [Stanford et al., 1995; Gillette and Nielsen-Preiss, 2004; Vaingankar et al., 2004]. Concerning drug treatments, cell cultures were grown to confluence and treated with 200 ng/ml cytochalasin D (CCD) or 1 μg/ml phalloidin (PHL; both from Sigma). Drugs were added to the media in dimethyl sulfoxide (DMSO). Control cultures received an equivalent amount of the solvent (0.05%, v/v).

ALKALINE PHOSPHATASE ACTIVITY ASSAY

Tissue non-specific alkaline phosphatase (TNAP) activity was measured using *p*-nitrophenyl phosphate as substrate at pH 10.4 and recording the absorbance at 420 nm ($\varepsilon_{p\text{-NP}}$ is equal to 18.8/mM/

cm) [Cyboron and Wuthier, 1981]. Enzyme units are micromole of *p*-nitrophenolate released per minute per milligram of protein.

IMMUNOFLUORESCENCE AND CONFOCAL MICROSCOPY

Saos-2 cells were cultured on cover slips at 37°C in 5% CO_2 humidified atmosphere. Cells (10^5) were washed with PD buffer (125 mM NaCl, 5 mM KCl, 10 mM $NaHCO_3$, 1 mM KH_2PO_4, 10 mM glucose, 1 mM $CaCl_2$, 1 mM $MgCl_2$, 20 mM HEPES, pH 6.9) and fixed with 3% (w/v) paraformaldehyde in PD buffer for 20 min at room temperature [Strzelecka-Kiliszek et al., 2008]. Fixed cells were incubated in 50 mM NH_4Cl in PD buffer (10 min, room temperature) and then permeabilized with 0.08% (v/v) Triton X-100 in PD buffer (5 min, 4°C). After additional washing, with PD buffer and Tris-buffered saline (TBS; 130 mM NaCl, 25 mM Tris–HCl, pH 7.5), cells were incubated with a blocking solution, 5% FBS in TBS (v/v) for 45 min at room temperature. Then, probes were incubated with mouse monoclonal anti-annexin A6 (anti-AnxA6; 1:100, v/v; Transduction Laboratories) or rabbit polyclonal anti-cofilin-1 antibody (1:50, v/v; Sigma), diluted in TBS containing 0.5% FBS (v/v) and 0.05% Tween-20 (v/v). After 1 h of incubation at room temperature, the cells were washed and incubated for 1 h at room temperature with goat anti-mouse IgG–fluorescein isothiocyanate (FITC; 1:200, v/v) or goat anti-rabbit IgG–tetramethylrhodamine isothiocyanate (TRITC) antibody (1:100, v/v; both from Sigma). After washing, the samples were mounted in Moviol 4-88/DABCO. Z-Section images were acquired with a TCS SP2 confocal microscope (Leica). Resting and stimulated cells were identified and each cell type was quantified as percentage of cell population.

CALCIUM NODULE DETECTION

Cell cultures were washed with phosphate-buffered saline (PBS) and stained with 0.5% (w/v) Alizarin Red-S (AR-S) in PBS (pH 5.0) for 30 min at room temperature [Vaingankar et al., 2004]. After washing four times with PBS to remove free calcium ions, the stained cultures were photographed. Then, cell cultures were destained with 10% (w/v) cetylpyridinium chloride in PBS pH 7.0 for 60 min at room temperature [Stanford et al., 1995]. AR-S concentration was determined by measuring the absorbance at 562 nm.

PREPARATION OF MICROVILLI AND MATRIX VESICLES

Both preparations were performed simultaneously with the same cell cultures according to Wu et al. [1993] for MV preparation and Jimenez et al. [2004] for microvilli preparation with slight modifications. The microvilli isolation was based on the property of $MgCl_2$ to precipitate membranous fractions except microvilli [Booth and Kenny, 1974]. It was suggested that aggregation of the membranous components occurs when bivalent cations establish cross-links between membranes. Microvilli do not aggregate because cross-linking by Mg^{2+} is established between contiguous anionic sites on the same microvillus. Saos-2 cell cultures were digested with 100 U/ml collagenase Type IA (Sigma) in Hank's balanced salt solution (HBSS; 5.4 mM KCl, 0.3 mM Na_2HPO_4, 0.4 mM KH_2PO_4, 0.6 mM $MgSO_4$, 137 mM NaCl, 5.6 mM D-glucose, 2.38 mM $NaHCO_3$, pH 7.4) at 37°C for 3 h. Then, cells were pelleted by centrifugation at 600*g* for 15 min. Supernatant was centrifuged at 20,000*g* for 20 min to sediment all the cell debris, nuclei, mitochondria and lysosomes. The supernatant was centrifuged again at 80,000*g* for 60 min yielding pellet containing MVs.

Cells were homogenized in 5 ml of sucrose buffer in the presence of the protease inhibitor cocktail (Sigma). The homogenate was then centrifuged twice at 10,000*g* for 15 min to sediment intact cells, cell debris, nuclei, mitochondria, and lysosomes. To separate the microvillar membranes from the basolateral plasma membranes, the supernatant was supplemented with 12 mM $MgCl_2$, stirred at 4°C for 20 min to induce basolateral membrane precipitation and centrifuged twice at 2,500*g* for 10 min to pellet aggregates of the basolateral membranes. Supernatant was centrifuged at 12,000*g* for 60 min to pellet microvilli. Fractions containing MVs and microvilli (8.6% sucrose, w/v) were overlaid on a sucrose step gradient made with 45%/37%/25% (w/v) sucrose and centrifuged at 90,000*g* for 5 h. The alkaline phosphatase activity was measured in fractions collected from the sucrose gradient. The 25% and 37% sucrose fractions were collected, mixed, diluted tenfold in HBSS, and centrifuged at 120,000*g* for 60 min. Protein concentration in the fractions was determined using the Bio-Rad Protein Assay.

SODIUM DODECYL SULFATE (SDS)–POLYACRYLAMIDE GEL ELECTROPHORESIS (PAGE) AND IMMUNOBLOT ANALYSIS

Proteins of each fraction were separated on 8, 10, or 12% (w/v) SDS–PAGE [Laemmli, 1970] and then electro-transferred (Mini-ProteanII™ Kit, Bio-Rad) onto nitrocellulose membranes (Hybond™-ECL™, Amersham Biosciences) according to Towbin et al. [1979]. Nitrocellulose membranes were blocked with 5% (w/v) milk in TBS for 1 h at room temperature. The nitrocellulose membranes were then incubated with primary antibodies, that is, mouse monoclonal anti-Na^+/K^+ ATPase (1:2,500; Abcam), mouse monoclonal anti-AnxA2 (1:2,500; Transduction Laboratories), mouse monoclonal anti-AnxA6 (1:5,000; Transduction Laboratories), mouse monoclonal anti-actin (1:2,000; Transduction Laboratories), or rabbit polyclonal anti-cofilin-1 (1:2,000; Sigma) prepared in 3% (w/v) milk in TBS supplemented with 0.05% (v/v) Tween-20 (TTBS) at 4°C overnight. Nitrocellulose membranes were washed several times with TTBS and then incubated with secondary antibodies, that is, sheep anti-mouse or anti-rabbit IgG conjugated with horseradish peroxidase (1:5,000; both from Amersham Biosciences) prepared in 3% (w/v) milk in TTBS. Finally, the membranes were washed and immunoreactive bands were visualized by using ECL reagents according to the manufacturer's instructions (Amersham Biosciences).

ELECTRON MICROSCOPY

Microvilli and MVs were washed in PD buffer and fixed with 3% (w/v) paraformaldehyde/1% (w/v) glutaraldehyde mixture in 100 mM sodium phosphate buffer (pH 7.2) for 1 h at room temperature [Strzelecka-Kiliszek et al., 2002]. After washing, samples were postfixed with 1% (w/v) osmium tetroxide in 100 mM sodium phosphate buffer (pH 7.2) for 20 min at room temperature and then dehydrated in a graded ethanol solution series at room temperature (25% (v/v) for 5 min, 50% (v/v) for 10 min, 75% (v/v) for 15 min, 90% (v/v) for 20 min, 100% (v/v) for 30 min). Then, samples were incubated in mixtures of the LR White resin/100% ethanol at volume ratios of 1:2 and 1:1 (30 min each, at room

temperature). Finally, samples were infiltrated twice with 100% (v/v) LR White resin (Polysciences) for 1 h at room temperature, moved to the gelatin capsule and polymerized at 56°C for 48 h. Sections (700 Å) were cut using an ultramicrotome LKB Nova, placed on formvar-covered and carbon-labeled 300 Mesh nickel grids (Agar Scientific Ltd.). The sample-covered grids were counterstained with 2.5% (w/v) uranyl acetate in ethanol for 1–1.5 h at room temperature. Finally, the grids were washed in 50% ethanol, then in water and stained with lead citrate for 2 min in NaOH atmosphere at room temperature, washed in water and dried [Strzelecka-Kiliszek et al., 2002]. The samples were observed by JEM-1200EX transmission electron microscopy (JEOL).

LIPID COMPOSITION

Total lipids were extracted according to Folch et al. [1957] with slight modifications. Total lipids of samples (15 μg of proteins) were extracted in chloroform/methanol (2:1, by volume). The organic phase was collected and washed three times in chloroform/methanol/H_2O (3:48:47, by volume). The lipid composition of samples was determined by thin layer chromatography (Balcerzak et al., 2007). Phospholipids were separated by migration up to 12 cm in ethyl acetate/1-propanol/chloroform/methanol/0.25% (w/v) KCl (25:25:25:10:9, by volume). Plates were completely dried. Then, other lipids were separated by a second migration up to 18 cm from the origin in heptane/isopropyl ether/acetic acid (75:21:4, by volume). After complete drying, lipid spots were visualized by incubating plates in 10% (w/v) $CuSO_4$/8% (v/v) H_2SO_4 for 10 min and heating at 180°C for 20 min. Chromatograms were scanned and analyzed by densitometry using the ImageJ software (NIH).

MINERALIZATION ASSAY

Aliquots of MVs and of each membranous fraction obtained from cell fractionation were diluted to a final protein concentration of 20 μg/ml in the mineralization buffer (100 mM NaCl, 12.7 mM KCl, 0.57 mM $MgCl_2$, 1.83 mM $NaHCO_3$, 0.57 mM Na_2SO_4, 3.42 mM NaH_2PO_4, 2 mM $CaCl_2$, 5.55 mM D-glucose, 63.5 mM sucrose, and 16.5 mM TES (pH 7.4). Samples were incubated at 37°C for 6 h. The mineral complexes were centrifuged at 3,000*g* for 10 min and washed several times with water. The final pellets were dried and incorporated by pressing into 100 mg of KBr. Mineral compositions were determined using a Nicolet 510M Infrared spectrometer (Nicolet) equipped with a DTGS detector; 64 interferograms were recorded at a 4 cm^{-1} optical resolution.

FACScan ANALYSIS

Dead cells were identified by the propidium iodide staining [Krishan, 1975]; 10^6 cells were incubated in 0.25% Trypsin (w/v), 0.03% EDTA (w/v; Sigma), washed twice in PBS and centrifuged at 600*g* for 10 min. Then, cells were suspended in 2 ml propidium iodide solution (50 g/ml propidium iodide in PBS), incubated for 5 min at room temperature and used directly for flow analysis. For evaluation of cell apoptosis by propidium iodide staining [Dressler, 1988], 10^6 cells were trypsinized and centrifuged at 2,500*g* for 5 min. Pellet was suspended in 0.2 ml PBS and added directly to 0.5 ml of pure cold ethanol (−20°C) and fixed overnight at −20°C. After fixation, cells were centrifuged at 1,500*g* for 5 min and the pellet was suspended in 0.5 ml propidium iodide solution (50 g/ml propidium iodide/0.1 mg/ml RNAse A/0.05% (v/v) Triton X-100 in PBS) and incubated for 45 min at 37°C. After incubation, cells were centrifuged at 1,500*g* for 5 min and the pellet was suspended in 2 ml of PBS and used for flow analysis. The propidium iodide fluorescence was monitored by FACScan flow cytometer (Becton-Dickinson) using Cell Quest software (Becton-Dickinson). Cell phenotypes were quantified in control and stimulated cell cultures every 3 days by FACScan analysis of the size (forward scatter of cells; FSC) and the granularity (side scatter of cells; SSC) of the cells. The total number of cells was determined from the light scatter FSC/SSC to distinguish differentiated cells from resting non-differentiated cells.

RESULTS

DIFFERENTIATION OF Saos-2 CELL AND MINERALIZATION

Saos-2 cells cultured in McCoy's 5A medium containing 0.9 mM Ca^{2+} and 4.2 mM P_i produced apparent calcium nodules characteristic of osteoblastic mineralization as detected by AR-S

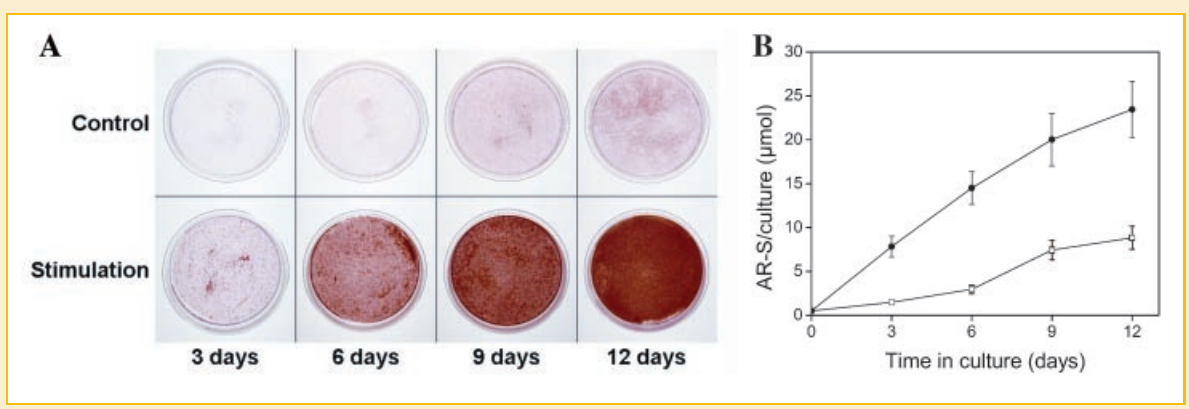

Fig. 1. Mineralization by Saos-2 cells. Saos-2 cells were incubated under normal conditions or stimulated with 50 μg/ml ascorbic acid (AA) and 7.5 mM β-glycerophosphate (β-GP) for the indicated time. A: Non-stimulated and stimulated cell cultures were stained with AR-S to detect calcium nodules and photographed. B: AR-S was solubilized in control (□) and stimulated (●) cell cultures by cetylpyridinium chloride and quantified at 562 nm (results are mean ± SD, n = 3).

staining (Fig. 1). AA and β-GP are two osteogenic factors commonly used to stimulate osteoblastic differentiation and mineralization [Gillette and Nielsen-Preiss, 2004; Vaingankar et al., 2004]. As expected, the mineral deposition was highly enhanced by the concomitant addition of 50 μg/ml AA and 7.5 mM β-GP in Saos-2 cell cultures (Fig. 1A). The non-stimulated Saos-2 cells produced within 9–12 days almost the same amount of calcium minerals (7.44 ± 1.12–8.826 ± 1.3 μmol of calcium mineral-bound AR-S) as stimulated Saos-2 cells within 3 days (7.832 ± 1.18 μmol of calcium mineral-bound AR-S) (Fig. 1A,B).

To evaluate the Saos-2 cell differentiation induced by AA and β-GP, cellular specific TNAP activity, MV biogenesis, AnxA6 localization, and morphology of untreated and treated cells were compared. TNAP is a metalloenzyme which provides P_i from various phosphorylated substrates during mineralization. Following the treatment with AA and β-GP, TNAP activity of Saos-2 cells increased with culture time in comparison to untreated cells (Fig. 2). AnxA6 belongs to a large family of Ca^{2+}- and lipid-binding proteins which are involved in maintaining Ca^{2+} homeostasis in bone cells and in extracellular MVs. Immunocytochemistry revealed that most of the control Saos-2 cells (96% in 3-day-cultures and 88% in 12-day-cultures (Fig. 3B, light gray), exhibited a fusiform or fibroblast-like shape with a characteristic cytoplasmic and membrane localization of AnxA6 typical for resting cells (Fig. 3A, control, arrows). Few cells were retracted, displayed cytoplasmic location of AnxA6 and became round with a characteristic plasma membrane-bound vesicles (Fig. 3A, control, asterisks). In comparison to control cultures, the population of Saos-2 cells exhibiting the latter phenotype (Fig. 3A, stimulation, asterisks) increased from 14% at day 3 to 57% at day 12 in the presence of AA and β-GP (Fig. 3C, dark gray), suggesting a differentiated state favoring mineralization. From the previous findings of Hale and Wuthier [1987] on hypertrophic chondrocytes, we hypothesized that Saos-2 cell apical microvilli facing the bone forming side are the precursors of MVs.

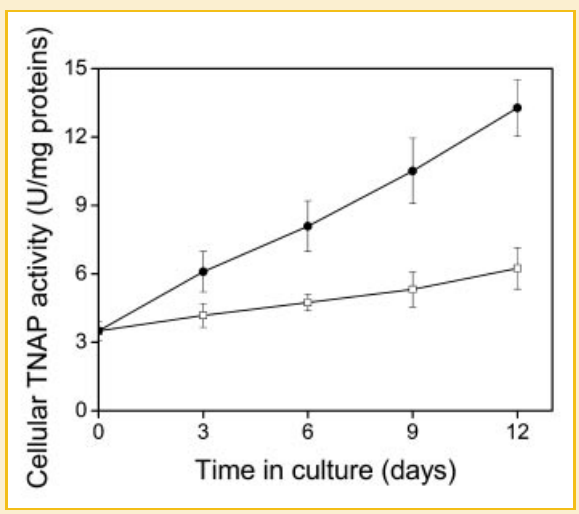

Fig. 2. Tissue non-specific alkaline phosphatase activity in Saos-2 cells. Saos-2 cells were grown under normal conditions (control) or were stimulated with 50 μg/ml AA and 7.5 mM β-GP for different incubation times. Tissue non-specific alkaline phosphatase activities of control (□) and stimulated (●) cells were measured every 3 days and are expressed as U/mg cellular protein (results are mean ± SD, n = 3).

Saos-2 CELL MICROVILLI AS PRECURSORS OF MATRIX VESICLES

Apical microvilli were isolated from Saos-2 cells according to the method of Jimenez et al. [2004] used to isolate microvilli from human placental syncytiotrophoblast. It consisted of the Mg^{2+}-induced precipitation in which non-microvillar membranes were aggregated and could be separated from vesicular microvilli by a low-speed centrifugation. Alkaline phosphatase is a well known and widely used apical marker of polarized cells [Moog and Grey, 1967; Kenny et al., 1969; Jimenez et al., 2004]. Alkaline phosphatase activity reached 110 ± 6 U/mg and was 13.1-fold enriched in the microvillar fraction, whereas the enrichment value of this enzyme was only 0.9 in the basolateral membrane fraction. The morphology of microvilli and MVs were compared by electron microscopy. MVs were identified as closed, spherical vesicle structures delimited by a characteristic trilaminar membrane described earlier for both epiphyseal cartilage [Anderson, 1969] and osteosarcoma cells [Fedde, 1992], with a diameter ranging from 100 to 500 nm (Fig. 4A,B). Microvilli were found to rearrange in round vesicle-like structures during preparation (Fig. 4C,D). The microvillar pellet was devoid of other subcellular contaminations as shown on the electron micrograph (Fig. 4C), suggesting a relatively pure fraction. These microvillar vesicles of 100–300 nm in diameter were delimited by a trilaminar membrane (Fig. 4C,D), showing a morphology similar to that of MVs. The ability of MVs, microvilli, and other membranous fractions from Saos-2 cells to mineralize was checked by incubating the samples in mineralization buffer at 37°C. After 6 h of incubation, the samples were centrifuged and the resulting pellets were analyzed by infrared spectroscopy. Under these conditions, both MVs and microvillar-rearranged vesicles were able to induce the formation of HA (Fig. 5). The amount of HA minerals formed by microvilli (Fig. 5, bottom trace) was lower than the amount produced by MVs (Fig. 5, middle trace). In contrast, no other fractions from Saos-2 cells produced HA.

Saos-2 CELL MICROVILLI AND MATRIX VESICLES EXHIBIT SIMILAR PROTEIN AND LIPID COMPOSITION

The lipid composition of MVs was compared with that of Saos-2 cell basolateral membranes and microvilli. The lipid content of MVs and that of microvilli were almost identical (Table I). In terms of lipid composition, MVs and microvilli were enriched in cholesterol (CHOL) and contained less TAGs and monoacylglycerols (MAGs) than the basolateral membrane fraction (Table I). Free CHOL constituted about 46.7% and 45.9% of total MV and microvillar lipids, respectively (Table I). The phospholipid composition of MVs and microvilli were nearly identical with ~36% of phosphatidylethanolamine (PE), ~26.5% of phosphatidylcholine (PC), ~3.5% of phosphatidic acid (PA), ~7% of phosphatidylinositol (PI), ~16.5% of phosphatidylserine (PS), and ~11% of sphingomyelin (SM) (Table II). The amounts of PE and PC in MVs and microvilli were lower, whereas the amounts of PS and SM were higher than those in basolateral membranes (Table II). Thus, MVs and microvilli obtained from Saos-2 cell cultures were enriched in CHOL, PS, and SM as in the case of MV produced by epiphyseal cartilage cells [Peress et al.,

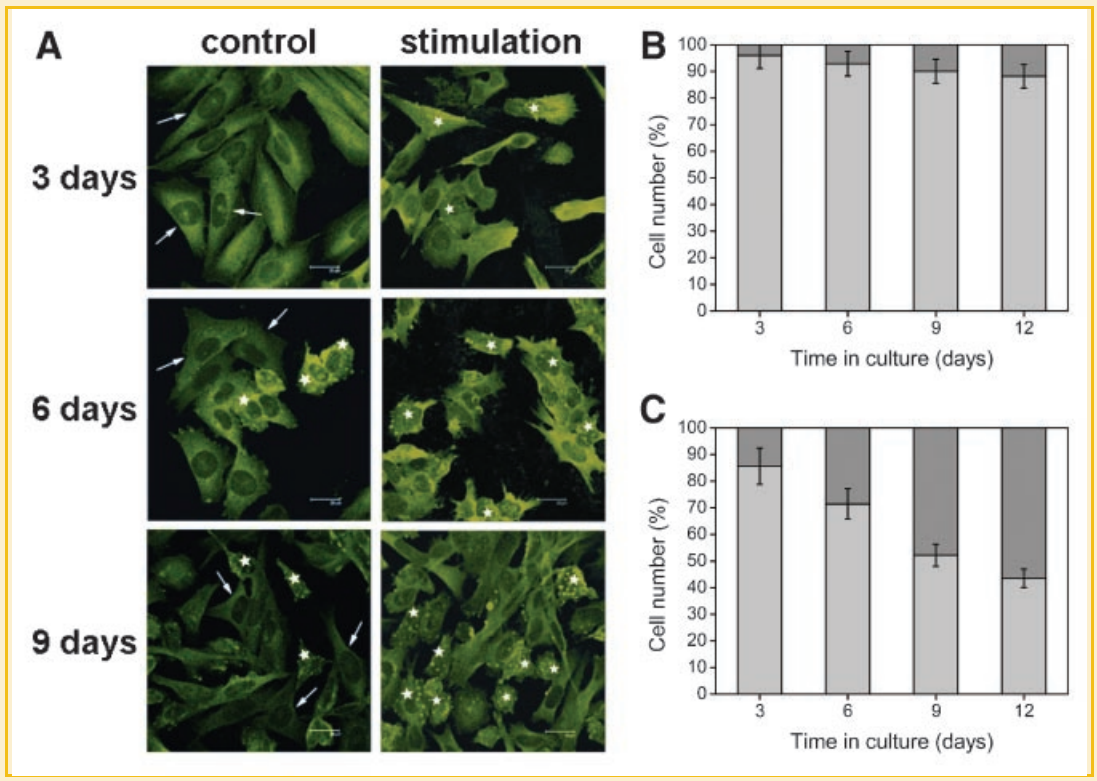

Fig. 3. Cellular morphology and annexin A6 distribution in Saos-2 cells. Saos-2 cells were grown under normal conditions (control) or were stimulated (stimulation) with 50 μg/ml AA and 7.5 mM β-GP for different incubation times directly on cover slips. AnxA6 was stained by immunocytochemistry and detected by confocal microscopy in control and stimulated Saos-2 cells cultured for 12 days. Two phenotypes were observed—resting cells (arrows) and differentiated cells (asterisks)—and quantified in control (B) and stimulated (C) cell cultures every 3 days and are presented as percentage of cell population (resting cells in light gray, differentiated cells in dark gray) (results are mean ± SD, n = 3).

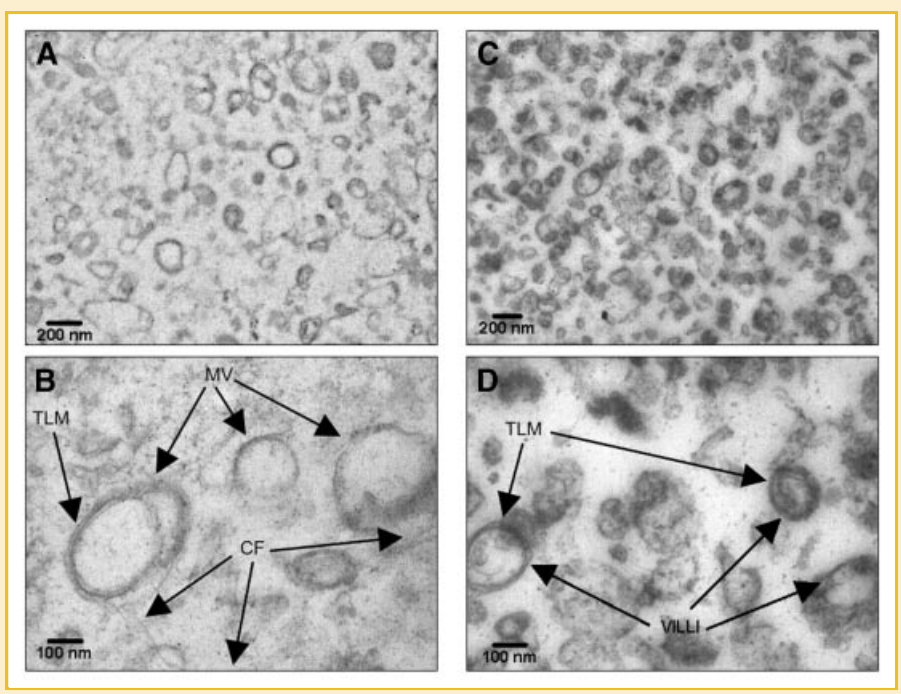

Fig. 4. Ultrastructural morphology of matrix vesicles and microvilli. MV, matrix vesicle (A,B); VILLI, microvilli (C,D); trilaminar membranes were evidenced (TLM); CF stands for collagen fibrils (magnifications: A and C, ×20,000; B and D, ×50,000).

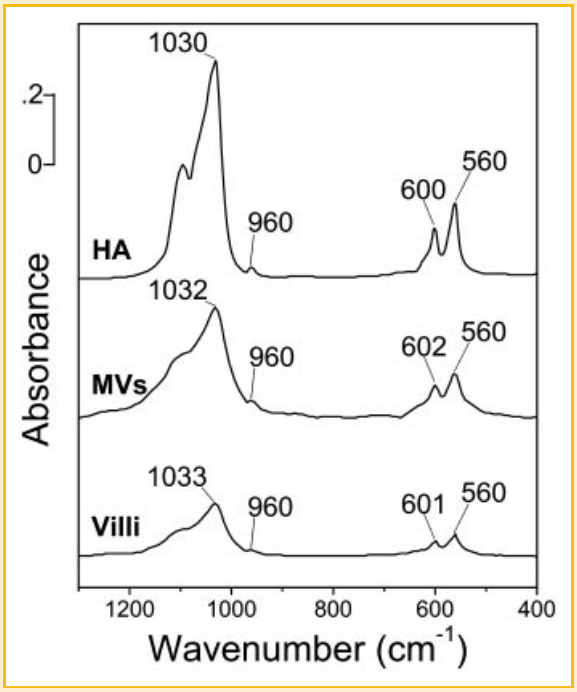

Fig. 5. Infrared spectra of minerals formed by matrix vesicles and microvilli. MVs and microvilli from Saos-2 cells were incubated at 37°C in mineralization buffer for 6 h then the minerals formed were collected, washed, and analyzed by infrared spectroscopy. Infrared spectrum of hydroxyapatite as control (HA); infrared spectrum of minerals formed by matrix vesicles (MVs) and by microvilli (Villi). Infrared spectra indicated that the minerals formed by MVs and microvilli were hydroxyapatite (typical infrared spectra out of two independent measurements).

1974; Wuthier, 1975b] or by hypertrophic chondrocytes [Glaser and Conrad, 1981].

The protein profile of MV was also compared with that of the other membranous fractions obtained from Saos-2 cells (Fig. 6A). The distribution of MV proteins (Fig. 6A, lane 6) closely resembled that of microvillar proteins (Fig. 6A, lane 4) but was different from that of other fractions (Fig. 6A, lanes 1–3 and 5). According to density tracings of the bands (data not shown), MV and microvillar protein profiles exhibited similar major bands with apparent molecular weights of: 85, 50, 45, 38, 36, 34, 33, 30, and 24 kDa (Fig. 6A, lanes 4 and 6). The immunodetection of Na^+/K^+ ATPase, AnxA6, and AnxA2 (Fig. 6B, lanes 4 and 5) indicated that these proteins were more enriched in microvilli and in MVs than in other fractions. TNAP activity was similar in microvilli and in MVs and higher than in other fractions (Fig. 6C, lanes 4 and 5). Thus, microvilli and MVs exhibited similar lipid and protein compositions.

TABLE I. Lipid Composition of Basolateral Membrane, Microvilli, and Matrix Vesicles

	BLM	Microvilli	MVs
% of total lipids			
TAGs	24.4 ± 1.6	14.8 ± 2.4	14.3 ± 1.2
FFAs	23.7 ± 1.9	23.6 ± 2.2	22.1 ± 1.0
CHOL	27.5 ± 1.5	45.9 ± 3.6	46.7 ± 3.2
DAGs	10.2 ± 1.2	10.2 ± 0.8	10.0 ± 0.9
MAGs	14.2 ± 1.0	5.5 ± 0.6	6.8 ± 0.9

BLM, basolateral membranes; Microvilli (from apical membranes); MVs, matrix vesicles; TAGs, triacylglycerols; FFAs, free fatty acids; CHOL, cholesterol; DAGs, diacylglycerols; MAGs, monoacylglycerols. Chromatogram scans were analyzed by densitometry using the ImageJ software. Values are expressed as apparent percentage of total lipids (results are mean ± SD, n = 3).

TABLE II. Phospholipid Composition of Basolateral Membrane, Microvilli, and Matrix Vesicles

	BLM	Microvilli	MVs
% of total phospholipids			
PE	38.1 ± 2.6	35.9 ± 2.5	35.8 ± 1.9
PA	5.1 ± 1.1	3.4 ± 0.3	3.5 ± 0.6
PI	9.9 ± 0.9	7.4 ± 1.5	6.7 ± 0.3
PS	9.9 ± 0.4	16.4 ± 1.2	16.3 ± 1.3
PC	32.6 ± 1.8	26.9 ± 2.2	26.2 ± 1.0
SM	4.4 ± 0.6	9.9 ± 0.9	11.5 ± 1.0

BLM, basolateral membranes; Microvilli (from apical membranes); MVs, matrix vesicles; PE, phosphatidylethanolamine; PA, phosphatidic acid; PI, phosphatidylinositol; PS, phosphatidylserine; PC, phosphatidylcholine; SM, sphingomyelin. Chromatogram scans were analyzed by densitometry using the ImageJ software. Values are expressed as apparent percentage of total phospholipids (results are mean ± SD, n = 3).

ROLE OF ACTIN DEPOLYMERIZATION IN MATRIX VESICLE RELEASE FROM Saos-2 CELLS

It has been reported that the release of MVs from cultured epiphyseal chondrocytes was correlated with changes in cellular actin distribution [Hale et al., 1983]. Therefore, we assessed the role of the actin network in MV formation by osteoblast-like Saos-2 cells. Cofilin-1 controls actin polymerization and depolymerization in a pH-sensitive manner [Pope et al., 2004]. The actin-binding protein co-localized with AnxA6 in control Saos-2 cells (Fig. 7A, control) and especially at the periphery of stimulated Saos-2 cells (Fig. 7A, stimulation). Moreover, immunodetection of cofilin-1 and actin revealed their presence in both MV and microvillar fractions (Fig. 7B). This suggested that actin microfilaments are involved in MV biogenesis. Therefore, we investigated whether actin polymerization or depolymerization could affect MV formation by monitoring the release of MVs from Saos-2 cells treated with actin-perturbing drugs: CCD or PHL which are known to inhibit microfilament assembly or disassembly, respectively [Hale and Wuthier, 1987]. In parallel, we examined the effects of AA and β-GP combined with CCD or PHL on cell viability (Fig. 8A) and cell apoptosis (Fig. 8B) by FACScan using propidium iodide staining. Six days of stimulation with AA and β-GP decreased cell viability from 70% to 55% (Fig. 8A). The rate of apoptosis in the case of stimulated cells was about 40%, that is, twice as high as for control cells (Fig. 8B). Furthermore, the stimulation of Saos-2 cells using these two osteogenic factors led to an increased release of MVs as shown in Figure 9. These findings suggested that AA and β-GP induced Saos-2 cells terminal differentiation and mineralization and this is consistent with the fact that mineralization is accompanied by apoptosis in growth plate chondrocytes [Anderson, 1995]. The viability of stimulated cells treated with PHL was not affected

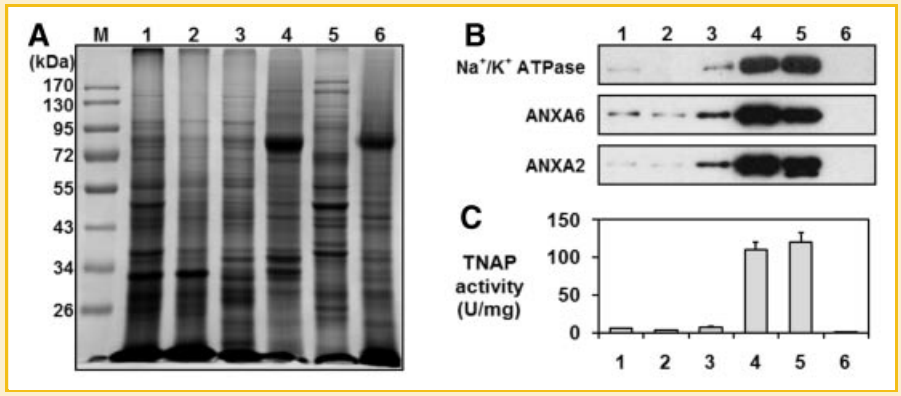

Fig. 6. Protein profiles of mineralizing Saos-2 cells, cell fractions and matrix vesicles. A: Protein profiles analyzed by 10% SDS–PAGE followed by Coomassie brilliant blue staining of intact Saos-2 cells (lane 1); cell debris, nuclei, mitochondria, lysosomes (lane 2); basolateral membranes (lane 3); microvilli (lane 4); microsomal and cytoplasmic fractions (lane 5); and matrix vesicles (lane 6; a typical gel out of five performed). B: Detection of Na^+/K^+ ATPase, AnxA6 and AnxA2 by Western blotting in intact Saos-2 cells (lane 1); cell debris, nuclei, mitochondria, lysosomes (lane 2); basolateral membranes (lane 3); microvilli (lane 4); matrix vesicles (lane 5); and final supernatant (lane 6; typical Western blot among five independent measurements). C: Alkaline phosphatase activity in intact Saos-2 cells (lane 1); cell debris, nuclei, mitochondria, lysosomes (lane 2); basolateral membranes (lane 3); microvilli (lane 4); matrix vesicles (lane 5); and final supernatant (lane 6) (results are mean ± SD, n = 10).

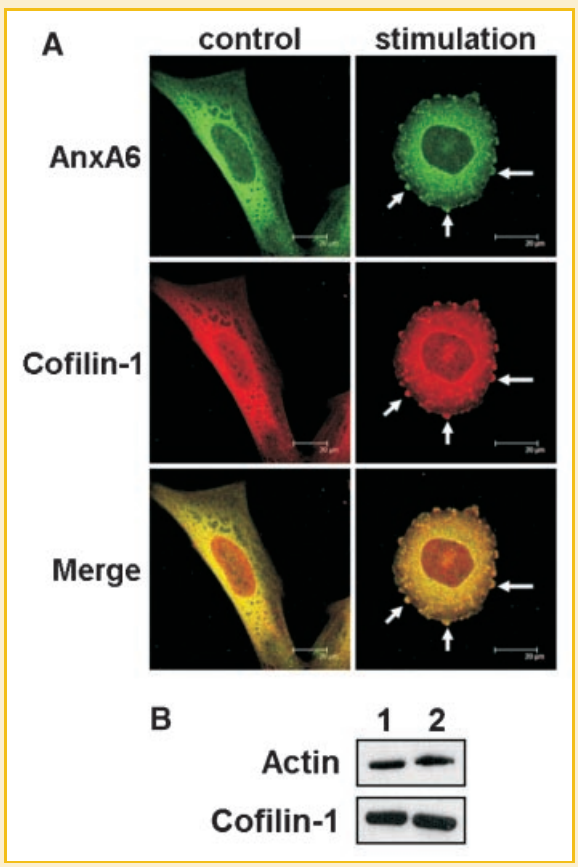

Fig. 7. Localization of AnxA6 and cofilin-1 in Saos-2 cells. Saos-2 cells were cultured under normal conditions or stimulated with 50 μg/ml AA and 7.5 mM β-GP for 6 days directly on cover slips. A: AnxA6 (green) and cofilin-1 (red) were stained by immunocytochemistry and detected by confocal microscopy in control and stimulated Saos-2 cells. Merge pictures (yellow) evidenced co-localization of AnxA6 and cofilin-1. Plasma membrane extrusions of stimulated Saos-2 cells are indicated with white arrows. B: Detection of actin and cofilin-1 by Western blotting in microvilli (lane 1) and matrix vesicles (lane 2) (n = 3).

(Fig. 8A) whereas treatment with CCD increased cell apoptosis from 40% to ~75% (Fig. 8B). PHL, which stabilizes actin microfilaments, did not affect significantly the production of MVs from stimulated Saos-2 cells while CCD, which inhibits the actin microfilament formation, enhanced MV formation (Fig. 9). The protein profiles of MVs from Saos-2 cells treated with CCD or PHL were identical except for high levels of actin in MVs obtained from cells treated with PHL (results not shown). This demonstrates that the mechanism of MV formation from Saos-2 cells involved actin microfilament depolymerization.

DISCUSSION

ASCORBIC ACID AND *B*-GLYCEROPHOSPHATE INDUCE SAOS-2 CELL DIFFERENTIATION AND RELEASE OF MATRIX VESICLES

Human osteosarcoma Saos-2 cells served as a model of pro-mineralizing cells, allowing us to determine the site of MV origin and the mechanisms leading to their release into the extracellular matrix. Osteoblast-mediated osteogenesis is divided into three main phases: (1) cell proliferation, (2) extracellular matrix deposition and maturation, and (3) mineralization [Owen et al., 1990; Manduca et al., 1997]. Saos-2 cells are characterized by the entire osteoblastic differentiation sequence from proliferation to mineralization [Hausser and Brenner, 2004]. They produce a collagenous extracellular matrix [McQuillan et al., 1995] and spontaneously release mineralization-competent MVs [Fedde, 1992]. AA and β-GP are commonly employed to stimulate osteoblastic differentiation and mineralization [Ecarot-Charrier et al., 1983; Nefussi et al., 1985; Quarles et al., 1992; Gillette and Nielsen-Preiss, 2004; Vaingankar et al., 2004]. In the present work, we used AA and β-GP simultaneously to stimulate Saos-2 cell-mediated mineralization (Fig. 1) associated with Saos-2 cell differentiation. TNAP activity was enhanced (Fig. 2), AnxA6 was enriched in the plasma membrane extensions (Fig. 3A) and Saos-2 cell became spherical (Fig. 3A). These findings are consistent with earlier reports on osteoblast differentiation induced by concomitant addition of AA and β-GP

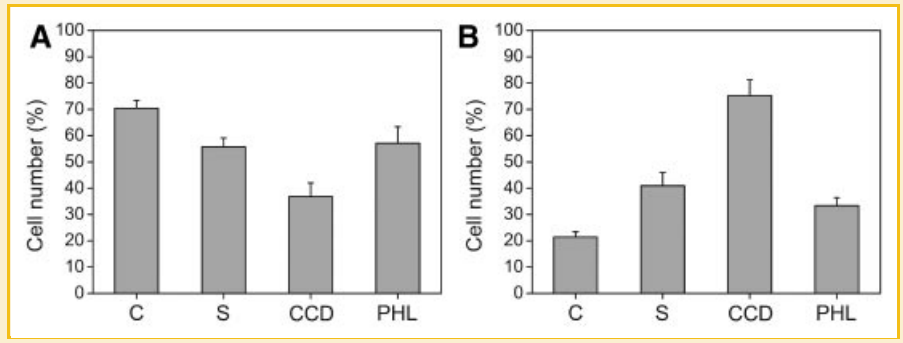

Fig. 8. Cell viability and apoptosis of Saos-2 cells. Saos-2 cells were maintained under normal conditions (C), stimulated (S) with 50 μg/ml AA and 7.5 mM β-GP or stimulated and treated with cytochalasin D (CCD) or phalloidin (PHL) for 6 days. Cell viability (A) and cell apoptosis (B) were determined by propidium iodide staining and FACScan analysis and are presented as percentage of cell number (results are mean ± SD, n = 3).

[Ecarot-Charrier et al., 1983; Nefussi et al., 1985; Quarles et al., 1992; Gillette and Nielsen-Preiss, 2004; Vaingankar et al., 2004]. AA is an exogenous osteogenic factor that stimulates the sequential differentiation of osteoblasts [Harada et al., 1991; Franceschi and Iyer, 1992; Quarles et al., 1992]. It has been shown that AA enhanced osteoblast proliferation through its stimulatory effect on collagen synthesis [Harada et al., 1991]. Franceschi and Iyer [1992] demonstrated that AA induced a temporal osteoblastic differentiation of MC3T3-E1 cells in culture. They showed that (1) collagen synthesis and deposition is stimulated by the increase of type I procollagen expression and processing of procollagens to collagens; (2) during the mineralization phase, TNAP expression and activity are enhanced, and osteocalcin synthesis is induced. These changes in marker gene expression were shown to be accompanied by changes in osteoblast shape from a fusiform to a cuboidal one [Quarles et al., 1992]. β-GP displays synergic action with AA in stimulating collagen accumulation and TNAP activity [Quarles et al., 1992]. It is also required for matrix mineralization as a source of P_i after hydrolysis by TNAP [Nefussi et al., 1985; Bellows et al., 1991; Anagnostou et al., 1996]. Moreover, P_i released from β-GP can act as a messenger for osteoblast differentiation [Conrads et al., 2005]. In addition to these effects of AA and β-GP, we found that they also stimulated the release of MVs from mineralizing Saos-2 cells (Fig. 9), which contributed to the increase of matrix mineralization. The stimulation with AA and β-GP induced a parallel significant increase of Saos-2 cell apoptosis (Fig. 8B). This was consistent with the fact that the mineralizing Saos-2 cells reached the terminal differentiation state and died by apoptosis. Since the local enrichment in AnxA6 in the plasma membrane could signal the origin of MVs, we decided to determine whether the apical microvilli of Saos-2 cells were the precursors of MVs in the plasma membrane.

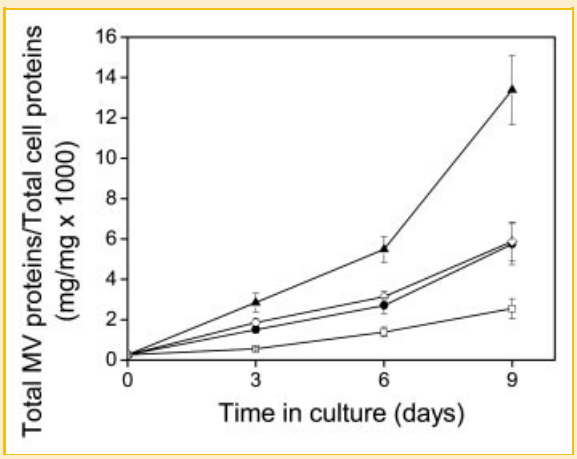

Fig. 9. Matrix vesicle formation from Saos-2 cells. Saos-2 cells were maintained under normal conditions (□), stimulated (●) with 50 μg/ml AA and 7.5 mM β-GP or stimulated and treated with cytochalasin D (▲) or phalloidin (◇) for different incubation times. MV release from Saos-2 cells was monitored as a ratio of total MV protein/total cellular protein (results are mean ± SD, n = 3).

MATRIX VESICLES ARE FORMED FROM SAOS-2 CELL MICROVILLI

A well-established method for the purification of microvilli from human placental syncytiotrophoblasts [Jimenez et al., 2004] served to purify microvilli from osteoblast-like Saos-2 cells. This method was very effective as revealed by the high enrichment in TNAP activity, a microvillar marker enzyme (Fig. 6C). The MV fraction was obtained simultaneously from cell cultures by collagenase digestion and several differential centrifugation steps. Microvilli and MVs were enriched in TNAP activity to a similar extent (Fig. 6C). During the preparation, microvilli formed vesicles as observed by electron microscopy (Fig. 4C,D), exhibiting identical spherical shapes within the same diameter range and analogous trilaminar membranous layers as in the case of MVs (Fig. 4A,B). Microvilli and MVs from Saos-2 cell cultures were able to form HA within 6 h in the presence of calcium ions and P_i, while other subcellular membranous fractions were not (Fig. 5). This functional similarity could originate from structural similarity. Therefore, the lipid and protein compositions of MVs and microvilli were compared. MVs were enriched in several proteins associated with mineralization (Fig. 6B, lane 5): annexins (AnxA2 and AnxA6) which are involved in Ca^{2+} homeostasis by mediating Ca^{2+} influx into MVs [Kirsch

et al., 2000; Wang and Kirsch, 2002; Wang et al., 2005]; Na^+/K^+ ATPase [Hsu and Anderson, 1996] and TNAP which promotes mineralization by increasing the local concentration of P_i and by decreasing the concentration of inorganic pyrophosphate (PP_i) [Anderson et al., 2004]. Microvilli were also enriched in these proteins (Fig. 6B, lane 4). In addition, the protein profiles of MVs and microvilli were similar (Fig. 6A, lanes 4 and 6). Negatively charged PS and annexins act as nucleators of Ca^{2+} and P_i [Wu et al., 1993, 1996; Genge et al., 2007, 2008]. MVs and microvilli exhibited a significantly higher enrichment in PS than the basolateral membrane of Saos-2 cells (Table II). The apparent lipid composition of MVs isolated from Saos-2 cell cultures was not exactly the same as that of MVs isolated from fetal epiphyseal cartilage [Peress et al., 1974; Wuthier, 1975b], growth plate cartilage [Wu et al., 2002; Genge et al., 2003] or hypertrophic chondrocyte cultures [Hale and Wuthier, 1987]. In comparison to the more recent and definitive lipid analyses of MVs [Wu et al., 2002; Genge et al., 2003], MVs isolated from Saos-2 cell cultures exhibited higher levels of free fatty acids (FFAs) and MAGs but a lower content of free CHOL (Table I), and higher levels of PE, PI and PS but a lower content of PC (Table II). However, MVs that originated from Saos-2 cells showed similar characteristics such as enriched contents of PS, SM and free CHOL (Tables I and II). The lipid and phospholipid compositions of isolated MVs and microvilli were very similar (Tables I and II). These findings are consistent with those reported by Hale and Wuthier [1987] showing that hypertrophic chondrocyte microvilli were the precursors of MVs. We found that cofilin-1, an actin binding protein, co-localized with AnxA6, especially in plasma membrane extrusions in the case of stimulated cells, and that cofilin-1 as well as actin were both present in microvilli and MVs (Fig. 7). Second, CCD, an inhibitor of actin microfilament polymerization, stimulated MV formation by Saos-2 cells but PHL which stabilized actin polymerization did not (Fig. 9). Our findings indicated that actin depolymerization was involved in the mineralization-competent MV formation and that the morphological and structural characteristics of MVs were similar to those of the apical microvilli suggesting that MVs derived from apical microvilli of mineralizing Saos-2 cells. This was also previously observed in the case of hypertrophic chondrocytes and it was concluded that MVs were derived from microvilli [Hale and Wuthier, 1987]. Taken together, these findings suggest that the microvillar origin of MV is common in various cell types such as osteoblast-like cells and hypertrophic chondrocytes. Pathological calcification is a process that has similarities with bone formation [Tanimura et al., 1983; Kirsch, 2007; van de Lest and Vaandrager, 2007]. Therefore, it is tempting to propose that the formation of MVs under physiological conditions may follow the same mechanisms that trigger vesicular release from the microvillar regions of other cells under pathological conditions leading to ectopic mineralization.

ACKNOWLEDGMENTS

We thank Dr. John Carew for correcting the English. This work was supported by a grant N301 025 32/1120 from the Polish Ministry of Science and Higher Education, by a Polonium grant (05819NF), by CNRS (France), and by the Rhône-Alpes region.

REFERENCES

Akisaka T, Shigenaga Y. 1983. Ultrastructure of growing epiphyseal cartilage processed by rapid freezing and freeze-substitution. J Electron Microsc 32: 305–320.

Akisaka T, Kawaguchi H, Subita GP, Shigenaga Y, Gay CV. 1988. Ultrastructure of matrix vesicles in chick growth plate as revealed by quick freezing and freeze substitution. Calcif Tissue Int 42:383–393.

Anagnostou F, Plas C, Nefussi JR, Forest N. 1996. Role of beta-GP-derived P_i in mineralization via ecto-alkaline phosphatase in cultured fetal calvaria cells. J Cell Biochem 62:262–274.

Anderson HC. 1969. Vesicles associated with calcification in the matrix of epiphyseal cartilage. J Cell Biol 41:59–72.

Anderson HC. 1995. Molecular biology of matrix vesicles. Clin Orthop Relat Res 314:266–280.

Anderson HC. 2003. Matrix vesicles and calcification. Curr Rheumatol Rep 5:222–226.

Anderson HC, Reynolds JJ. 1973. Pyrophosphate stimulation of calcium uptake into cultured embryonic bones. Fine structure of matrix vesicles and their role in calcification. Dev Biol 34:211–227.

Anderson HC, Stechschulte DJ, Collins DE, Jacobs DH, Morris DC, Hsu HHT, Redford PA, Zeiger S. 1990. Matrix vesicle biogenesis in vitro by rachitic and normal rat chondrocytes. Am J Pathol 136:391–398.

Anderson HC, Sipe JB, Hessle L, Dhanyamraju R, Atti E, Camacho NP, Millán JL. 2004. Impaired calcification around matrix vesicles of growth plate and bone in alkaline phosphatase-deficient mice. Am J Pathol 164:841–847.

Balcerzak M, Hamade E, Zhang L, Pikula S, Azzar G, Radisson J, Bandorowicz-Pikula J, Buchet R. 2003. The roles of annexins and alkaline phosphatase in mineralization process. Acta Biochim Pol 50:1019–1038.

Balcerzak M, Pikula S, Buchet R. 2007. Phosphorylation-dependent phospholipase D activity of matrix vesicles. FEBS Lett 580:5676–5680.

Bellows CG, Aubin JE, Heersche JN. 1991. Initiation and progression of mineralization of bone nodules formed in vitro: The role of alkaline phosphatase and organic phosphate. Bone Miner 14:27–40.

Booth AG, Kenny AJ. 1974. A rapid method for the preparation of microvilli from rabbit kidney. Biochem J 142:575–581.

Borg TK, Runyan RB, Wuthier RE. 1978. Correlation of freeze-fracture and scanning electron microscopy of epiphyseal chondrocytes. Calcif Tissue Res 26:237–241.

Borg TK, Runyan R, Wuthier RE. 1981. A freeze-fracture study of avian epiphyseal cartilage differentiation. Anat Rec 199:449–457.

Brighton CT, Hunt RM. 1976. Histochemical localization of calcium in growth plate mitochondria and matrix vesicles. Fed Proc 35:143–147.

Buckwalter JA, Cooper RR. 1987. Bone structure and function. Instr Course Lect 36:27–28.

Cecil RN, Anderson HC. 1978. Freeze-fracture studies of matrix vesicle calcification in epiphyseal growth plate. Metab Bone Dis 1:89–97.

Conrads KA, Yi M, Simpson KA, Lucas DA, Camalier CE, Yu LR, Veenstra TD, Stephens RM, Conrads TP, Beck GR, Jr. 2005. A combined proteome and microarray investigation of inorganic phosphate-induced pre-osteoblast cells. Mol Cell Proteomics 4:1284–1296.

Cyboron GW, Wuthier RE. 1981. Purification and initial characterization of intrinsic membrane-bound alkaline phosphatase from chicken epiphyseal cartilage. J Biol Chem 256:7262–7268.

Dressler LG. 1988. DNA flow cytometry and prognostic factors in 1331 frozen breast cancer specimens. Cancer 61:420–427.

Ecarot-Charrier B, Glorieux FH, Van Der Rest M, Pereira G. 1983. Osteoblasts isolated from mouse calvaria initiate matrix mineralization in culture. J Cell Biol 96:639–643.

Fedde KN. 1992. Human osteosarcoma cells spontaneously release matrix-vesicle-like structures with the capacity to mineralize. Bone Miner 17:145–151.

Folch J, Lees M, Sloane Stanley GH. 1957. A simple method for the isolation and purification of total lipids from animal tissues. J Biol Chem 226:497–509.

Franceschi RT, Iyer BS. 1992. Relationship between collagen synthesis and expression of the osteoblast phenotype in MC3T3-E1 cells. J Bone Miner Res 7:235–246.

Garimella R, Bi X, Camacho N, Sipe JB, Anderson HC. 2004. Primary culture of rat growth plate chondrocytes: An in vitro model of growth plate histotype, matrix vesicle biogenesis and mineralization. Bone 34:961–970.

Genge BR, Wu LN, Wuthier RE. 2003. Separation and quantification of chicken and bovine growth plate cartilage matrix vesicle lipids by high-performance liquid chromatography using evaporative light scattering detection. Anal Biochem 322:104–115.

Genge BR, Wu LN, Wuthier RE. 2007. In vitro modeling of matrix vesicle nucleation: Synergistic stimulation of mineral formation by annexin A5 and phosphatidylserine. J Biol Chem 282:26035–26045.

Genge BR, Wu LN, Wuthier RE. 2008. Mineralization of biomimetic models of the matrix vesicle nucleation core: Effect of lipid composition and modulation by cartilage collagens. J Biol Chem 283:9737–9748.

Gillette JM, Nielsen-Preiss SM. 2004. The role of annexin 2 in osteoblastic mineralization. J Cell Sci 117:441–449.

Glaser JH, Conrad HE. 1981. Formation of matrix vesicles by cultured chick embryo chondrocytes. J Biol Chem 256:12607–12611.

Golub EE, Schattschneider SC, Berthold P, Burke A, Shapiro IM. 1983. Induction of chondrocyte vesiculation in vitro. J Biol Chem 258:616–621.

Hale JE, Wuthier RE. 1987. The mechanism of matrix vesicle formation. Studies on the composition of chondrocyte microvilli and on the effects of microfilament-perturbing agents on cellular vesiculation. J Biol Chem 262: 1916–1925.

Hale JE, Chin JE, Ishikawa Y, Paradiso PR, Wuthier RE. 1983. Correlation between distribution of cytoskeletal proteins and release of alkaline phosphatase-rich vesicles by epiphyseal chondrocytes in primary culture. Cell Motil 3:501–512.

Harada S, Matsumoto T, Ogata E. 1991. Role of ascorbic acid in the regulation of proliferation in osteoblast-like MC3T3-E1 cells. J Bone Miner Res 6:903–908.

Hausser HJ, Brenner RE. 2004. Low doses and high doses of heparin have different effects on osteoblast-like Saos-2 cells in vitro. J Cell Biochem 91: 1062–1073.

Hsu HHT, Anderson HC. 1996. Evidence of the presence of a specific ATPase responsible for ATP-initiated calcification by matrix vesicles isolated from cartilage and bone. J Biol Chem 271:26383–26388.

Ilvesaro J, Metsikkö K, Väänänen K, Tuukkanen J. 1999. Polarity of osteoblasts and osteoblast-like UMR-108 cells. J Bone Miner Res 14:1338–1344.

Jimenez V, Henriquez M, Llanos P, Riquelme G. 2004. Isolation and purification of human placental plasma membranes from normal and pre-eclamptic pregnancies: A comparative study. Placenta 25:422–437.

Kardos TB, Hubbard MJ. 1982. Are matrix vesicles apoptotic bodies? Prog Clin Biol Res 101:45–60.

Kenny AJ, George SG, Aparicio SG. 1969. The localization of peptidases in microvilli from the brush border of the proximal renal tubule of the rabbit. Biochem J 115:18P.

Kirsch T. 2007. Physiological and pathological mineralization: A complex multifactorial process. Curr Opin Orthop 18:434–443.

Kirsch T, Harisson G, Golub EE, Nah HD. 2000. The roles of annexins and types II and X collagen in matrix vesicle-mediated mineralization of growth plate cartilage. J Biol Chem 275:35577–35583.

Kirsch T, Wang W, Pfander D. 2003. Functional differencies between growth plate apoptotic bodies and matrix vesicles. J Bone Miner Res 18:1872–1881.

Krishan A. 1975. Rapid flow cytometric analysis of mammalian cell cycle by propidium iodide staining. J Cell Biol 66:188–193.

Laemmli UK. 1970. Cleavage of structural proteins during the assembly of the head of bacteriophage T4. Nature 227:680–685.

Manduca P, Palermo C, Caruso C, Brizzolara A, Sanguineti C, Filanti C, Zicca A. 1997. Rat tibial osteoblasts III: Propagation in vitro is accompanied by enhancement of osteoblast phenotype. Bone 21:31–39.

Marks SC, Popoff SN. 1988. Bone cell biology: The regulation of development, structure and function in the skeleton. Am J Anat 183:1–44.

McQuillan DJ, Richardson MD, Bateman JF. 1995. Matrix deposition by a calcifying human osteogenic sarcoma cell line (Saos-2). Bone 16:415–426.

Moog F, Grey RD. 1967. Spatial and temporal differentiation of alkaline phosphatase on the intestinal villi of the mouse. J Cell Biol 32:C1–C5.

Morris DC, Masuhara K, Takaoka K, Ono K, Anderson HC. 1992. Immunolocalization of alkaline phosphatase in osteoblasts and matrix vesicles of human fetal bone. Bone Miner 19:287–298.

Nefussi JR, Boy-Lefevre ML, Boulekbache H, Forest N. 1985. Mineralization in vitro of matrix formed by osteoblasts isolated by collagenase digestion. Differentiation 29:160–168.

Owen TA, Aronow M, Shalhoub V, Barone LM, Wilming L, Tassinari MS, Kennedy MB, Pockwinse S, Lian JB, Stein GS. 1990. Progressive development of the rat osteoblast phenotype in vitro: Reciprocal relationships in expression of genes associated with osteoblast proliferation and differentiation during formation of the bone extracellular matrix. J Cell Physiol 143:420–430.

Peress NS, Anderson HC, Sajdera SW. 1974. The lipids of matrix vesicles from bovine fetal epiphyseal cartilage. Calcif Tissue Res 14:275–281.

Pope BJ, Zierler-Gould KM, Kühne R, Weeds AG, Ball LJ. 2004. Solution structure of human cofilin: Actin binding, pH sensitivity, and relationship to actin-depolymerizing factor. J Biol Chem 279:4840–4848.

Quarles LD, Yohay DA, Lever LW, Caton R, Wenstrup RJ. 1992. Distinct proliferative and differentiated stages of murine MC3T3-E1 cells in culture: An in vitro model of osteoblast development. J Bone Miner Res 7:683–692.

Rabinovitch AL, Anderson HC. 1976. Biogenesis of matrix vesicles in cartilage growth plates. Fed Proc 35:112–116.

Stanford CM, Jacobson PA, Eanes ED, Lembke LA, Midura RJ. 1995. Rapidly forming apatitic mineral in an osteoblastic cell line (UMR 106-01 BSP). J Biol Chem 270:9420–9428.

Strzelecka-Kiliszek A, Kwiatkowska K, Sobota A. 2002. Lyn and Syk kinases are sequentially engaged in phagocytosis mediated by FcR. J Immunol 169:6787–6794.

Strzelecka-Kiliszek A, Buszewska ME, Podszywalow-Bartnicka P, Pikula S, Otulak K, Buchet R, Bandorowicz-Pikula J. 2008. Calcium- and pH-dependent localization of annexin A6 isoforms in Balb/3T3 fibroblasts reflecting their potential participation in vesicular transport. J Cell Biochem 104:418–434.

Tanimura A, McGregor DH, Anderson HC. 1983. Matrix vesicles in atherosclerotic calcification. Proc Soc Exp Biol Med 172:173–177.

Thouverey C, Bleicher F, Bandorowicz-Pikula J. 2007. Extracellular ATP and its effects on physiological and pathological mineralization. Curr Opin Orthop 18:460–466.

Towbin H, Staehelin T, Gordon J. 1979. Electrophoretic transfer of proteins from polyacrylamide gels to nitrocellulose sheets: Procedure and some applications. Proc Natl Acad Sci USA 76:4350–4354.

Vaingankar SM, Fitzpatrick TA, Johnson K, Goding JW, Maurice M, Terkeltaub R. 2004. Subcellular targeting and function of osteoblast nucleotide pyrophosphatase phosphodiesterase 1. Am J Physiol Cell Physiol 286: C1177–C1187.

Van de Lest CHA, Vaandrager AB. 2007. Mechanisms of cell-mediated mineralization. Curr Opin Orthop 18:434–443.

Wang W, Kirsch T. 2002. Retinoic acid stimulates annexin-mediated growth plate chondrocyte mineralization. J Cell Biol 157:1061–1069.

Wang W, Xu J, Kirsch T. 2005. Annexin V and terminal differentiation of growth plate chondrocytes. Exp Cell Res 305:156–165.

Wu LN, Yoshimori T, Genge BR, Sauer GR, Kirsch T, Ishikawa Y, Wuthier RE. 1993. Characterization of the nucleational core complex responsible for mineral induction by growth plate cartilage matrix vesicles. J Biol Chem 268: 25084–25094.

Wu LN, Ishikawa Y, Sauer GR, Genge BR, Mwale F, Mishima H, Wuthier RE. 1995. Morphological and biochemical characterization of mineralizing primary cultures of avian growth plate chondrocytes: Evidence for cellular processing of Ca^{2+} and P_i prior to matrix mineralization. J Cell Biochem 57:218–237.

Wu LN, Genge BR, Sauer GR, Wuthier RE. 1996. Characterization and reconstitution of the nucleational complex responsible for mineral formation by growth plate cartilage matrix vesicles. Connect Tissue Res 35:309–315.

Wu LN, Genge BR, Kang MW, Arsenault AL, Wuthier RE. 2002. Changes in phospholipid extractability and composition accompany mineralization of chicken growth plate cartilage matrix vesicles. J Biol Chem 277:5126–5133.

Wuthier RE. 1975a. Effect of phospholipids on the transformation of amorphous calcium phosphate to hydroxapatite in vitro. Calcif Tissue Res 19:197–210.

Wuthier RE. 1975b. Lipid composition of isolated epiphyseal cartilage cells, membranes and matrix vesicles. Biochim Biophys Acta 409:128–143.

Wuthier RE, Majeska RJ, Collins GM. 1977. Biosynthesis of matrix vesicles in epiphyseal cartilage. I. In vivo incorporation of ^{32}P orthophosphate into phospholipids of chondrocyte, membrane, and matrix vesicle fractions. Calcif Tissue Res 23:135–139.